Clinical Cancer Research

High ALK receptor tyrosine kinase expression supersedes ALK mutation as a determining factor of an unfavorable phenotype in primary neuroblastoma

Johannes H. Schulte, Hagen S. Bachmann, Bent Brockmeyer, et al.

Clin Cancer Res Published OnlineFirst June 1, 2011.

High *ALK* receptor tyrosine kinase expression supersedes *ALK* mutation as a determining factor of an unfavorable phenotype in primary neuroblastoma

Johannes H. Schulte[1], Hagen S. Bachmann[2], Bent Brockmeyer[1], Katleen DePreter[3], André Oberthür[4], Sandra Ackermann[4], Yvonne Kahlert[4], Kristian Pajtler[1], Jessica Theissen[4], Frank Westermann[5], Jo Vandesompele[3], Frank Speleman[3], Frank Berthold[4], Angelika Eggert[1], Benedikt Brors[6], Barbara Hero[4], Alexander Schramm[1], Matthias Fischer[4]*

[1]Department of Pediatric Oncology and Hematology, University Children's Hospital, Essen, Germany
[2]Institute of Pharmacogenetics, University Hospital Essen, Germany
[3]Center for Medical Genetics, Ghent University Hospital, Belgium
[4]Department of Pediatric Oncology and Hematology, University Children's Hospital, and Center for Molecular Medicine Cologne (CMMC), Cologne, Germany
[5]Department of Tumor Genetics (B030), German Cancer Research Center, Heidelberg, Germany
[6]Department of Theoretical Bioinformatics (B080), German Cancer Research Center, Heidelberg, Germany

*Corresponding author:
Dr. Matthias Fischer, MD
University Children's Hospital of Cologne
Department of Pediatric Oncology
Kerpener Str. 62
50924 Cologne, Germany
Tel.: +49 221 478 6816
Fax: +49 221 478 4689
e-mail: matthias.fischer@uk-koeln.de

This work was supported by grants from the *Deutsche Krebshilfe* (grant 50–2719-Fi1 and 106847), the German Ministry for Education and Research (BMBF) through the National Genome Research Network 2 (NGFN2, grant 01GS0456) and National Genome Research Network plus (NGFNplus, grants 01GS0895 to MF and 01GS0896 to BB), the *Auerbach-Stiftung*, the Competence Network Pediatric Oncology and Hematology (KPOH), the *Fördergesellschaft Kinderkrebs-Neuroblastom-Forschung e.V.*, and the Fund for Scientific Research, Flanders (KDP).

Running title: *ALK* expression and mutation in neuroblastoma

Key words: neuroblastoma, ALK, mutation, expression, molecular and clinical phenotype

Statement of Translational Relevance

Activating mutations of the anaplastic lymphoma kinase (ALK) gene have recently been identified in 8% of primary neuroblastoma. This finding has focused intense interest in the development of innovative treatment strategies for high-risk neuroblastoma patients using inhibitors directed toward activated ALK, and first clinical trials with ALK inhibitory drugs have been initiated. In this study, we show that primary neuroblastomas with *ALK* mutations invariably exhibit elevated *ALK* expression levels. We furthermore demonstrate that tumors with *ALK* mutations resemble neuroblastomas with high-level wild-type *ALK* expression in their global gene expression patterns, and that patients of these two subtypes are characterized by similar prognostic marker profiles and unfavorable clinical courses. These data indicate that high ALK expression levels mediate similar molecular functions in primary neuroblastoma with mutated or wild-type *ALK*, suggesting that ALK inhibitory drugs should be evaluated in second-line treatment strategies of all high-risk neuroblastoma patients with elevated *ALK* expression.

Abstract

Purpose: Genomic alterations of the anaplastic lymphoma kinase (ALK) gene have been postulated to contribute to neuroblastoma pathogenesis. This study aimed to determine the interrelation of *ALK* mutations, *ALK* expression levels and clinical phenotype in primary neuroblastoma.

Experimental Design: The genomic *ALK* status and global gene expression patterns were examined in 263 primary neuroblastomas. Allele-specific *ALK* expression was determined by cDNA cloning and sequencing. Associations of genomic *ALK* alterations and *ALK* expression levels with clinical phenotypes and transcriptomic profiles were compared.

Results: Non-synonymous point mutations of *ALK* were detected in 21/263 neuroblastomas (8%). Tumors with *ALK* mutations exhibited about 2-fold elevated median *ALK* mRNA levels in comparison to tumors with wild-type *ALK*. Unexpectedly, the wild-type allele was preferentially expressed in 12/21 mutated tumors. Whereas survival of patients with *ALK* mutated tumors was significantly worse as compared to the entire cohort of wild-type *ALK* patients, it was similarly poor in patients with wild-type *ALK* tumors in which *ALK* expression was as high as in *ALK* mutated neuroblastomas. Global gene expression patterns of tumors with *ALK* mutations or with high-level wild-type *ALK* expression were highly similar, and suggested that ALK may be involved in cellular proliferation in primary neuroblastoma.

Conclusions: Primary neuroblastomas with mutated *ALK* exhibit high *ALK* expression levels and strongly resemble neuroblastomas with elevated wild-type *ALK* expression levels in both their clinical and molecular phenotypes. These data suggest that high levels of mutated and wild-type *ALK* mediate similar molecular functions that may contribute to a malignant phenotype in primary neuroblastoma.

Introduction

Neuroblastoma is a pediatric tumor of the developing sympathetic nervous system accounting for about 8% of childhood cancers (1). The biological and clinical behavior of neuroblastoma is remarkably heterogeneous. While fatal progression of the disease occurs frequently in children with disseminated tumors, spontaneous regression or differentiation into benign ganglioneuroma is regularly observed in infants. The genetic etiology and molecular mechanisms of the different neuroblastoma subtypes have remained enigmatic. Yet, it has been demonstrated in recent years that aggressive neuroblastomas and those with the capacity to regress spontaneously differ in a number of molecular characteristics (2), suggesting that they represent different subtypes of the disease (3).

In 2008, it has been reported that potentially activating mutations in the anaplastic lymphoma kinase (*ALK*) gene may account for most cases of familiar neuroblastoma and a fraction of sporadic neuroblastomas (4-7). ALK is a receptor tyrosine kinase involved in neuronal differentiation (8, 9), and pleiotrophin (PTN) and midkine (MDK) have been suggested to act as ligands for ALK in humans (10). Inappropriate ALK expression due to chromosomal translocations has been observed in several types of cancer, and constitutive ALK activity has been shown to induce malignant transformation both *in vitro* and *in vivo* (11), thus representing a potential molecular target for selective tyrosine kinase inhibitors (11, 12). In neuroblastoma, somatically acquired genomic amplification and mutation of *ALK* occur in 1-4% and 6-8% of primary tumors, respectively (4-7, 13). In addition, it was shown in cell line models that *ALK* mutations are likely oncogenic events that confer malignant properties to the cells. The association of *ALK* mutations with the clinical phenotype of the disease has remained contradictory. Some authors suggested an association of *ALK* mutations with an aggressive phenotype (4, 5), whereas others described *ALK* mutations in the entire spectrum of sporadic (6, 13) and familiar neuroblastoma (7). In addition to genomic alterations of *ALK*, elevated *ALK* expression levels have previously been reported for

neuroblastoma (14, 15). However, the interrelation of *ALK* mutations, *ALK* expression levels and clinical phenotype has remained elusive.

In this work, we determined the contribution of genomic *ALK* alterations and *ALK* expression to the clinical and molecular phenotypes of primary neuroblastomas. We assessed the frequency of genomic *ALK* alterations in a large and representative neuroblastoma cohort, evaluated the relationship of *ALK* mutations and *ALK* expression levels, and investigated the association of genomic and transcriptomic *ALK* status with global gene expression patterns of the tumors as well as prognostic markers and clinical outcome of the patients.

Material and Methods

Patients

The study comprised primary neuroblastoma samples from 263 patients (Supplementary Table 1). All patients were enrolled in the German Neuroblastoma trials with informed consent. Patients' age at diagnosis ranged from 0 to 295 months (median age, 15 months). Median follow-up for patients without fatal events was 84 months. Five-year event-free survival (EFS) of the total cohort was 0.69±0.03 and 5-year overall survival (OS) 0.80±0.03. Stage was classified according to the International Neuroblastoma Staging System (INSS): stage 1, n=68; stage 2, n=43; stage 3, n=41; stage 4, n=80; stage 4S, n=31. The distribution of age and stage in this cohort was representative of the German NB97 trial. Chromosomal alterations were determined by fluorescence *in situ* hybridization and defined according to the guidelines of the European Neuroblastoma Quality Assessment Group (16). *MYCN* was amplified in 45 (17.1%) and non-amplified in 215 cases (81.7%; missing *MYCN* status, n=3). Loss of chromosome 1p or 11q was observed in 61 (23.2%) and 59 tumors (22.4%), respectively, while 194 and 192 tumors had a normal 1p (73.8%) and a normal 11q status (73.0%), respectively (non-informative cases for 1p and 11q, n=8 and n=12, respectively). A favorable and an unfavorable histology according to the Shimada system (17) were diagnosed in 148 (56.3%) and 88 tumors (33.5%), respectively (missing information, n=27). Response to treatment was defined according to the revised criteria of the International Neuroblastoma Response Criteria (INRC).

Sample preparation

Tumor samples were checked by a pathologist for at least 60% tumor content. DNA was isolated from approximately 20 mg of snap-frozen tissue obtained before cytotoxic treatment using the Puregene Blood Core Kit B (Qiagen, Hilden, Germany). Total RNA was isolated from 30 to 60 mg of the same snap-frozen tumors using the FastPrep FP120 cell disruptor (Qbiogene-Inc, Carlsbad, CA) and the TRIzol reagent (Invitrogen, Karlsruhe, Germany). RNA

integrity was assessed using the 2100 Bioanalyzer (Agilent Technologies, Waldbronn, Germany) considering only samples with an RNA Integrity Number of at least 7.5.

Sequencing of DNA and cDNA

For sequencing of the *ALK* gene, exons encoding the kinase domain (i.e., exons 20, 21-22, 23, 24 and 25) were PCR amplified using the primers generated by De Brouwer et al. for exons 21-22 (13) and by Chen et al. for all other exons (4) (Supplementary Table 2). PCR conditions were as follows: 95°C for 3 min, 40 cycles of 95°C for 30 s, 60°C for 30 s and 72°C for 30 s, and a final extension step at 72°C for 5 min. PCR reactions were performed in 20 µl with illustra Taq polymerase and PCR buffer according to the manufacturer's protocol (GE Healthcare, Munich, Germany). Purification and Sanger sequencing of the PCR products was performed by the Eurofins MWG Operon Sequencing Service (Eurofins MWG Operon, Ebersberg, Germany).

Allele-specific expression was determined by amplification of transcript fragments encompassing the respective point mutations using RT-PCR, followed by cloning and sequencing. PCR fragments were cloned into plasmid vectors using the TOPO TA cloning kit (Invitrogen), and sequenced using the BigDye Terminator sequencing kit (Applied Biosystems, Darmstadt, Germany). Primer sequences for amplification are available from the authors upon request.

DNA copy number quantification

ALK copy number status was determined using real-time quantitative PCR with *TNFRSF17* and *SDC4* as normalizing reference genes and normal human genomic DNA (Roche Diagnostics, Mannheim, Germany) as calibrator sample (18). DNA from NB1, a neuroblastoma cell line with known *ALK* amplification, was used as a positive control. Primer sequences can be found in RTprimerDB (http://medgen.ugent.be/rtprimerdb, *TNFRSF17*, ID 14; *SDC4*, ID 15; *ALK*, ID 8117) (19). Five µl amplification mixtures contained 2-12 ng of DNA, 1x SYBR green I mastermix (Eurogentec S.A., Seraing, Belgium) and 250 nM of each

primer. PCR reactions were performed in a 384-well plate on a LightCycler 480 (Roche). The cycling conditions comprised 10 min polymerase activation at 95°C and 45 cycles of 15 s at 95°C and 30 s at 60°C, followed by a dissociation curve analysis from 60 to 95°C in order to verify amplification specificity. The haploid *ALK* copy number for each sample was calculated using the real-time PCR data analysis software qbase^{PLUS} (http://www.qbaseplus.com) (20). Haploid copy numbers >4 were considered as amplification.

Gene expression analyses

Gene expression profiles were generated as dye-flipped dual-color duplicates using customized 11K oligonucleotide-microarrays as described (21). The *ALK* gene was represented by probe A_23_P324304. As a reference, pooled total RNA from 100 primary neuroblastomas was used. Data pre-processing, quality control analyses and normalization were performed as described. All raw and normalized microarray data are available at the ArrayExpress database (http://www.ebi.ac.uk/arrayexpress; Accession: E-TABM-38, E-MTAB-161).

For real-time quantitative RT-PCR (RT-qPCR), single-stranded cDNA was generated from total RNA using the Superscript II First-Strand Synthesis System (Invitrogen). RT-qPCR was performed on an ABI PRISM 7700 Sequence Detection System (Applied Biosystems) with SYBR Green chemistry using the standard curve method. To prevent amplification of contaminating genomic DNA, primer sequences were selected allowing intron-spanning amplification (Supplementary Table 2). PCR reactions were run in duplicates for each sample and as triplicates for determination of standard curves. For normalization, the expression level of the target gene was divided by the geometric mean of expression levels of the control genes *HPRT1* and *SDHA* as described (22).

Western blot analyses

To analyze expression of proteins, tumor tissue or cell lines were lysed on ice for 30 min in RIPA buffer (50 mM HEPES, pH 7.4, 150 mM NaCl, 0.1% SDS, 1% Triton X-100, and 1%

NP-40) supplemented with complete Protease Inhibitor cocktail (Roche) and Phos-Stop (Roche). After centrifugation of lysates, 20 µg of protein were separated by sodium dodecyl sulfate (SDS)-polyacrylamide gel electrophoresis (PAGE) with 8% or 4-12% Tris-glycine gels and transferred to nitrocellulose membranes by tank blotting or semi-dry blotting. The membranes were blocked with either 5% dry milk powder or 5% BSA in 0.05% Tween-20/PBS before incubation with monoclonal primary antibodies (rabbit anti-human ALK, dilution 1:500; rabbit anti-human phospho-(y1604)-ALK, dilution 1:500; rabbit anti-human phospho-STAT3, dilution 1:2000, rabbit anti-human phospho-AKT, dilution 1:500, rabbit anti-human phospho-ERK1/2, dilution 1:1000; all Cell Signaling Technology, Danvers, MA) and horseradish peroxidase-labeled secondary goat anti-rabbit antibody (dilution 1:1000; Dako, Glostrup, Denmark). The antigen-antibody complex was detected with the ECL Prime western blotting detection kit (GE Healthcare).

Cell lines and cell culture

The human neuroblastoma cell line SK-N-AS, which has been described to express low levels of wild-type (WT) *ALK* (7), was grown as monolayer in RPMI 1640 supplemented with 10% FCS, L-glutamine and antibiotics. The cell line was authenticated by STR genotyping (DSMZ, Braunschweig, Germany). SK-N-AS cells were transfected by electroporation with pcDNA6/TR (Invitrogen) harboring the gene coding for the tetracyclin repressor, and single cell clones were raised by limited dilution and antibiotic selection (blasticidine). The cDNA encoding *ALK*(F1174L) was synthesized (Genescript, USA), with HindIII and NotI restriction sites flanking the kinase domain without altering the protein sequence. In addition, the cDNA was flanked by attL sites for subsequent Gateway cloning (Invitrogen, Carlsbad, CA). Alternative kinase cassettes, representing the WT sequence or a kinase domain haboring the R1275Q mutation, were synthesized and introduced by cloning via the HindIII and NotI restriction sites. WT *ALK* as well as *ALK*(F1174L) or *ALK*(R1275Q) cDNA were subcloned into pT-REx-DEST30 (Invitrogen), a vector for Tet-conditional expression, by a Gateway Cloning Reaction (Invitrogen). SK-N-AS-TR were transfected by electroporation with pT-REx-

DEST30-wtALK, pT-REx-DEST30-ALK(F1174L), pT-REx-DEST30-ALK(R1275Q) or pT-REx-DEST30-GFP. Single cell clones were raised by selection with antibiotics G418 and blasticidine and by limited dilution. For conditional ALK or GFP expression, cells were treated with tetracyclin (1 µg/ml) for 24h before being lysed on ice in RIPA buffer (50 mM HEPES, ph7.4, 150 mM NaCl, 0.1% SDS, 1% Triton X-100, and 1% NP-40) supplemented with complete Protease Inhibitor cocktail (Roche) and Phos-Stop (Roche).

Statistical analyses

Associations of *ALK* mutations or *ALK* expression levels with prognostic markers were determined by U-test or chi-square-test were appropriate. Allele-specific expression in tumors with mutated *ALK* was assessed by Wilcoxon-test. Kaplan-Meier estimates for EFS and OS were calculated and compared by log-rank test. Recurrence, progression and death from disease were considered as events. For multivariate analysis, Cox proportional hazards regression model based on EFS and OS was applied. The factors *ALK* mutation (mutated vs. wild-type) and *ALK* expression (continuous) were fitted by stepwise-backward selection. The likelihood ratio test p-value for inclusion was <0.05 and for exclusion >0.1.

Principal component analysis (PCA) and analysis of variance (ANOVA) of gene expression data was performed using Rosetta Resolver Software. To test for global gene expression differences between *ALK*-WT^{high} tumors, *ALK*-WT^{low} tumors and tumors with *ALK* mutation, differences between group centroids were calculated as described (23, 24). In brief, normalized intensity values from all probes were averaged in each group to yield group centroids. The Euclidean distance between these vectors was calculated and compared to centroid distances obtained from 1000 random permutations of the group labels. The number of differentially expressed genes was calculated with either pair-wise t tests or by one-way ANOVA over all three groups; for this, only genes (probes) in a list with a false discovery rate <0.05 were considered, after correction for multiple testing by the Benjamini-Hochberg method. All calculations except ANOVA were carried out in R version 2.9.0 (http://www.R-project.org) with extension package limma (version 2.18.0).

To identify gene expression patterns associated with either mutated *ALK* or WT *ALK* in primary neuroblastoma, the correlation of *ALK* expression levels with all genes represented on the microarray was examined. Thresholds for high and low correlation were defined using quantile-quantile plots of all correlation coefficients against a theoretical normal distribution. According to this procedure, thresholds for genes positively or negatively correlated with *ALK* expression in *ALK* mutated tumors and in WT *ALK* tumors were defined as $r \geq 0.5$ or $r \leq -0.5$ and $r \geq 0.25$ or $r \leq -0.25$, respectively. Lists of genes positively or negatively correlated with *ALK* were subjected to over-representation analysis of Gene Ontology (GO) categories by GOstats (25). Over-representation analysis of Gene Ontology categories was determined by Fisher's exact test ($p<0.05$ after Benjamini-Hochberg correction for multiple testing) using R version 2.11.0 with extension packages GOstats (v. 2.14.0) and GO.db (version 2.4.1). Correction for multiple testing was done by package multtest (v. 2.4.0).

Results

Association of genomic alterations of ALK with clinical variables in primary neuroblastoma

The prevalence of genomic *ALK* mutations was determined in a representative cohort of 263 primary neuroblastomas. Genomic amplification of wild-type (WT) *ALK* was observed in 2/263 tumors. Point mutations were detected in 23/263 cases, 21 of which were heterozygous non-synonymous mutations corresponding to an overall prevalence of 8.0% (Table 1). Nine different nucleotide exchange mutations were observed, including three which had not been described previously. The most common mutations were F1174L (n=5) and R1275Q (n=8) as reported previously (4-7, 13).

Next, the association of genomic *ALK* alterations with patient clinical courses and prognostic markers was assessed. Both tumors with *ALK* amplification showed *MYCN* amplification and loss of chromosome 1p (Table 1), in line with previous observations (4-7). One of these patients succumbed to disease, while the other is currently in complete remission. Non-synonymous *ALK* mutation ($ALK^{mutated}$) was not associated with stage 4 disease (p=0.805), the genomic status of chromosome 1p (p=0.283) or the Shimada classification (p=0.195). Patients having $ALK^{mutated}$ tumors tended to be older at diagnosis than those without mutations (p=0.064). Although not statistically significant (p=0.132), the prevalence of *ALK* mutations was twice as high in *MYCN* amplified tumors (n=6, 14%) as in tumors without *MYCN* amplification (n=15, 7%). Only a single $ALK^{mutated}$ tumor showed loss of 11q, which is a significant inverse correlation of these genetic variables (p=0.032). Whereas EFS and OS were significantly worse in $ALK^{mutated}$ patients than in patients with WT *ALK* (Fig. 1), there was no significant difference in the clinical courses of patients with different types of *ALK* mutations (Supplementary Figure 1).

Genomic ALK alterations are associated with elevated ALK expression levels

To examine the influence of genomic *ALK* alterations on *ALK* transcript levels, relative *ALK* mRNA expression levels were determined in all 263 tumors using microarrays (21, 26), and

validated in 81 samples by RT-qPCR (Supplementary Figure 2). *ALK*^{mutated} neuroblastomas exhibited significantly higher *ALK* transcript levels than tumors with WT *ALK* (p<0.001). The median expression in tumors with *ALK* amplification and *ALK* mutation was about 20-fold and 2-fold higher than in WT *ALK* tumors, respectively (Fig. 2A, Supplementary Table 3). In contrast, *ALK* mRNA levels did not differ between subgroups with different *ALK* mutations (F1174L *vs.* R1275Q *vs.* other mutation, p=0.345, Fig. 2A). In addition, high *ALK* mRNA expression correlated well with strong ALK protein expression in most primary tumors as determined by Western blot analysis (Supplementary Fig. 3).

Unexpectedly, sequencing of cloned *ALK* transcript fragments from *ALK*^{mutated} neuroblastomas revealed a significant preponderance of WT allele expression (WT *vs.* mutated allele expression in the entire *ALK*^{mutated} cohort, p=0.034). In particular, the WT allele was preferentially expressed (≥2-fold higher expression than the mutated allele) in all tumors with the F1174L mutation (Table 1). A more heterogeneous pattern of *ALK* allele expression was detected in the subgroup of neuroblastomas with R1275Q or other mutations. Allele-specific expression was not associated with any particular clinical parameter. Together, these results suggest that either low levels of mutated ALK are sufficient to contribute to the tumor phenotype, or that ALK expression levels rather than the mutation status represent a determining factor for neuroblastoma tumor behavior.

High ALK expression correlates with an adverse neuroblastoma phenotype independent of the genomic ALK status

Based on these findings, we hypothesized that high *ALK* expression levels should correlate with an adverse phenotype of neuroblastoma irrespective of the genomic *ALK* status. Indeed, *ALK* transcript levels were significantly higher in subgroups characterized by adverse prognostic markers than in favorable subgroups in the WT *ALK* cohort (stage 4 *vs.* stages 1-3 and 4S, age >18 months *vs.* <18 months, 1p-loss *vs.* 1p normal, unfavorable *vs.* favorable Shimada classification, p<0.001 each; amplified *vs.* non-amplified *MYCN*, p=0.011; 11q-loss *vs.* 11q normal, p=0.010). Moreover, *ALK* expression was significantly associated with poor

patient survival in a univariate Cox regression model using *ALK* mRNA levels as a continuous variable (EFS, p=0.005, hazard ratio [HR] 3.27, 95% confidence interval [CI] 1.43-7.47; OS, p=0.003, HR 5.13, CI 1.72-15.30). Accordingly, WT *ALK* expression correlated inversely with patient survival in subgroups created by subdivision according to percentiles of *ALK* transcript levels (<25th percentile, *ALK*-WT^{low}; >25th and <50th percentile, *ALK*-WT$^{intermediate\text{-}low}$; >50th and <75th percentile, *ALK*-WT$^{intermediate\text{-}high}$; >75th percentile, *ALK*-WT^{high}; n=60 each; Fig. 2B and 3). To determine whether *ALK* expression and *ALK* mutation status are independent prognostic markers, the two variables *ALK* expression (continuous) and genomic *ALK* status (mutated *vs.* WT) were analyzed in multivariate Cox regression models. Here, *ALK* expression, but not *ALK* mutation was independently associated with patient outcome (Supplementary Table 4). In addition, the prognostic value of *ALK* mutation status and *ALK* expression levels was evaluated in the context of the current German risk estimation system, which utilizes the variables stage, age, *MYCN* status and 1p status. In these multivariate analyses, stage, age and 1p status were independent prognostic variables in the models based on EFS, whereas inhomogeneous results were obtained in the forward and backward models based on OS (probably due to too few events to assess 6 prognostic markers in this cohort; data not shown).

Moreover, the distributions of prognostic markers and clinical courses of patients with *ALK*-WT^{high} and *ALK*^{mutated} neuroblastomas were compared, since these cohorts showed similar *ALK* expression levels (Fig. 2B). The subgroups did not differ in age (p=0.624), stage (p=0.565), *MYCN* status (p=1.0), classification according to our gene expression-based classifier (21) (p=0.519) or 1p-status (p=0.604). A significant difference was observed only in the prevalence of 11q-loss (35.1% and 4.8% of the *ALK*-WT^{high} and *ALK*^{mutated} cases, respectively; p=0.008). In addition, clinical courses of patients with *ALK*^{mutated} and *ALK*-WT^{high} tumors were similar in both the entire cohort and after excluding *MYCN* amplified neuroblastomas (Fig. 3, Supplementary Fig. 4). Taken together, these data indicate that *ALK*^{mutated} and *ALK*-WT^{high} neuroblastomas exhibit highly similar clinical phenotypes.

Author Manuscript Published OnlineFirst on June 1, 2011; DOI:10.1158/1078-0432.CCR-10-2809
Author manuscripts have been peer reviewed and accepted for publication but have not yet been edited.

ALK^{mutated} *and ALK-WT*^{high} *neuroblastomas show similar molecular phenotypes*

To investigate transcriptomic characteristics of tumors with and without *ALK* mutations, we performed principal component analyses (PCA) using global gene expression information of all samples. Here, *ALK*-WT^{low} and *ALK*-WT^{high} tumors formed separate subgroups, while *ALK*^{mutated} tumors showed a similar distribution to *ALK*-WT^{high} tumors in both the entire cohort and after excluding *MYCN* amplified neuroblastomas (Fig. 4, Supplementary Fig. 5). Of note, those four *ALK*^{mutated} neuroblastomas showing lower *ALK* expression levels than *ALK*-WT^{high} tumors were more closely associated with the *ALK*-WT^{low} subgroup (Supplementary Fig. 5). To validate these observations, the *ALK*-WT^{low}, *ALK*-WT^{high} and *ALK*^{mutated} subgroups were compared in a pair-wise manner using analysis of centroid distances, ANOVA and t-test statistics (Table 2). Both *ALK*^{mutated} and *ALK*-WT^{high} tumors differed significantly from *ALK*-WT^{low} tumors ($p<0.001$) by analysis of centroid distances. In contrast, *ALK*-WT^{high} and *ALK*^{mutated} tumors appeared to be more similar ($p=0.027$). Accordingly, only few transcripts were differentially expressed between these two subgroups, whereas multiple genes were differentially expressed between *ALK*-WT^{low} and *ALK*-WT^{high} or *ALK*^{mutated} neuroblastomas.

To gain insight into the molecular mechanisms by which ALK may exert its effects on neuroblastoma pathogenesis, the phosphorylation status of ALK targets was examined in neuroblastoma cell lines carrying either WT or mutated *ALK* transgenes and in primary tumors. In the cell line model, strong phosphorylation of ALK itself was observed in F1174L mutants upon *ALK* induction, while weak to modest ALK phosphorylation occurred in WT clones and R1275Q mutants, respectively (Supplementary Fig. 6). In addition, ALK induction resulted in a discrete to moderate increase of p-STAT3 and p-ERK/1/2 in clones FL8 and FL1 harboring the F1174L mutation, while it had no effect on target phosphorylation in all other clones. In primary tumors, the levels of phosphorylated ALK targets were highly heterogeneous, and neither correlated with genomic alterations of *ALK* nor *ALK* expression (Supplementary Fig. 3). Together, these data suggest that activation of known ALK targets may be limited and significantly modulated by other factors in neuroblastoma *in vivo*. In

addition, analysis of transcript levels of the putative ALK ligands PTN and MDK revealed a discrete correlation of *MDK* with *ALK* expression, and slightly elevated *MDK* expression levels in *ALK*-WT^{high} tumors (Supplementary Fig. 7). The significance of this finding for neuroblastoma pathogenesis, however, remains uncertain.

To identify gene expression patterns associated with either mutated or WT *ALK* in primary neuroblastoma, the correlation of *ALK* expression with all genes represented on the microarray was examined in these subgroups. In total, 1733 genes were positively or negatively correlated with *ALK* expression in *ALK*^{mutated} tumors (Supplementary Table 5A), while 823 genes were correlated with *ALK* expression in WT *ALK* tumors (Supplementary Table 5B). Of note, the overlap of genes correlated with *ALK* expression in WT *ALK* and *ALK*^{mutated} tumors was exceptionally high (57%), and the direction of correlation was concordant (i.e., either positive or negative) for all these genes. Over-representation analysis of Gene Ontology categories revealed 59 GO categories significantly enriched among the genes positively correlated with *ALK* expression in tumors with WT *ALK* (Supplementary Table 6). These categories were related to cell cycle regulation, DNA replication, cell division, DNA repair and protein ubiquitinylation. In contrast, no GO category was significantly enriched for genes negatively correlated with *ALK* expression. In *ALK*^{mutated} tumors, 21 and 14 significantly enriched GO categories were found among the genes positively and negatively correlated with *ALK* expression, respectively. Notably, 18/21 (86%) of the categories enriched for positively correlated genes were also found among the 59 categories identified in WT *ALK* tumors. These findings support the hypothesis that high expression levels of WT *ALK* and high expression levels of mutated *ALK* have a similar impact on the molecular phenotype in primary neuroblastoma which may be related to cellular proliferation.

Discussion

Activating mutations and amplification of the *ALK* gene have been described to contribute to neuroblastoma pathogenesis (4-7). The interrelation of *ALK* mutations, *ALK* expression and clinical phenotype, however, has remained ambiguous so far. In this study, heterozygous missense mutations were detected in 21/263 tumors (8%), which is in line with frequencies reported previously (4-7, 13). In contrast to results of a recent meta-analysis (13), *ALK* mutations were associated with a worse EFS and OS in this study (Fig. 1). This discrepancy might be attributed to a different composition of the cohort in the study of De Brouwer, which contained substantially more high-risk patients. It must be stressed, though, that *ALK* mutations did not show a clear correlation with established prognostic markers in both studies, and that mutations were detected in patients throughout the whole spectrum of the disease in the present survey, including spontaneously regressing stage 4S patients (NB068 and NB052).

The relationship of *ALK* mutation and *ALK* expression has been investigated in neuroblastoma cell lines (5, 7) and in small patient cohorts (27, 28) so far. In this study, we demonstrate that mutations in the ALK tyrosine kinase domain are invariably associated with elevated *ALK* transcript levels in primary neuroblastoma. While the molecular mechanism of this finding remains unclear, it appears reasonable to assume that mutated *ALK* promotes its own expression via a feed-forward regulatory loop. A similar mechanism has been described for the ErbB2 receptor tyrosine kinase in breast cancer, which actively induces its own over-expression (29). Yet, the observation of elevated *ALK* expression levels in a substantial fraction of WT *ALK* tumors may suggest additional mechanisms promoting *ALK* expression. Alternatively, somatic mutations may be preferentially acquired in *ALK* loci showing high transcriptional activity. Together, results from our study and others substantiate that *ALK* expression is regularly elevated in $ALK^{mutated}$ primary neuroblastoma (27, 28), however, the molecular mechanisms underlying this phenomenon are still to be elucidated.

The association of WT *ALK* expression levels with the clinical phenotypes of neuroblastoma has remained uncertain to date (13-15, 28, 30). Here, we show that elevated *ALK* mRNA levels are associated with an unfavorable neuroblastoma phenotype independent of the genomic *ALK* status, indicating a role of elevated *ALK* expression in the development of aggressive neuroblastoma. Patients with *ALK*-WT^{high} tumors in which *ALK* expression was as high as in *ALK*^{mutated} tumors had a similar poor outcome as those with *ALK* mutations, indicating that both patient subgroups may benefit from ALK-targeted therapies. However, analogous to the broad range of clinical phenotypes of patients with mutated *ALK*, we observed both patients with fatal outcome in the *ALK*-WT^{low} subgroup and patients with spontaneously regressing tumors (n=4) in the *ALK*-WT^{high} subgroup. Accordingly, neither *ALK* mutation status nor *ALK* expression turned out to be independent prognostic markers in multivariate analyses considering variables of the current German risk estimation system. In light of the results of this study and others (13) as well as the high prognostic accuracy of recently published complex DNA- or RNA-based prognostic classifiers (21, 26, 31-33), it remains questionable whether *ALK* mutation status or expression level will be useful for risk estimation of neuroblastoma patients in the future.

Comparison of *ALK*^{mutated} and *ALK*-WT^{high} neuroblastomas revealed highly similar prognostic marker profiles and clinical outcomes in these patients. In line with this observation, global gene expression patterns of these two subgroups were also alike. In addition, more than half the genes that correlated with *ALK* expression in WT *ALK* tumors were also associated with *ALK* expression in mutated tumors. Gene Ontology categories of transcripts positively correlated with *ALK* expression were enriched for functions related to cellular proliferation in both *ALK*^{mutated} and WT *ALK* tumors. Together, these data strongly suggest that high expression levels of WT *ALK* and mutated *ALK* have similar effects on the neuroblastoma biological phenotype that may be related to tumor growth.

Unexpectedly, we observed that levels of phosphorylated ALK targets were highly heterogeneous in primary tumors and did neither correlate with ALK expression nor with the *ALK* mutation status of the tumor, indicating substantial influences of other pathways on the

activation of these proteins in primary neuroblastomas. Moreover, the WT *ALK* allele was found to be preferentially expressed in many primary *ALK*^{mutated} neuroblastomas. It appears unlikely that this finding was due to contaminating *ALK* transcripts from stromal cells, since only samples with a tumor content of >60% were analyzed, and non-malignant cells in neuroblastomas have been shown to be ALK-negative (28). Allelic variations in gene expression have been shown to contribute to human variability and disease including cancer (34-37). To our knowledge, however, this is the first report on preferential WT allele expression of an oncogene harboring putatively activating mutations. While the underlying processes of allele-specific expression are largely unexplored, a *cis* effect of the *ALK* mutation such as reduced RNA stability of the affected *ALK* transcript might contribute to this unexpected observation (37). Besides the molecular mechanisms of allele-specific expression, it remains to be determined whether the mutated ALK protein, the enhanced ALK expression or both confer the functions of this tyrosine kinase in *ALK*^{mutated} neuroblastoma.

Taken together, this study demonstrates that primary neuroblastomas with mutated *ALK* invariably exhibit high *ALK* expression levels with preferential expression of the WT allele in some cases. *ALK*^{mutated} tumors strongly resemble *ALK*-WT^{high} neuroblastomas in both their clinical phenotypes and their transcriptomic profiles. The unfavorable patient outcome of these subgroups and the *ALK* associated gene expression patterns concordantly point to a pathogenetic role of ALK in malignant progression of both WT and mutant *ALK* primary neuroblastoma. These findings are in line with *in vitro* studies demonstrating that knock-down or inhibition of ALK using siRNA or inhibitory small molecules, respectively, resulted in anti-tumorigenic effects in neuroblastoma cell lines with high ALK expression levels irrespective of the presence of activating mutations (6, 7, 28). In contrast, neuroblastoma cell lines with low-level ALK expression were not susceptible to ALK knock-down (e.g., cell lines SK-N-DZ, NGP), ALK inhibition (e.g., NB5, NB-INT1) or both (SK-N-AS) in these studies. The consistency of the results from both *in vivo* and *in vitro* studies suggest the level of expression rather than the activating mutation as the primary mediator of the molecular functions of ALK in established neuroblastoma. These data, however, do not rule out the

possibility that activating *ALK* mutations may play a critical role in neuroblastoma initiation and early development, which remains to be addressed in future studies.

Acknowledgements

We thank Andrea Odersky for excellent technical assistance and Dr. Kathy Astrahantseff for critical reading of the manuscript.

References

1. Maris JM, Hogarty MD, Bagatell R, Cohn SL. Neuroblastoma. Lancet 2007;369: 2106-20.
2. Oberthuer A, Theissen J, Westermann F, Hero B, Fischer M. Molecular characterization and classification of neuroblastoma. Future Oncol 2009;5: 625-39.
3. Brodeur GM. Neuroblastoma: biological insights into a clinical enigma. Nat Rev Cancer 2003;3: 203-16.
4. Chen Y, Takita J, Choi YL*, et al.* Oncogenic mutations of ALK kinase in neuroblastoma. Nature 2008;455: 971-4.
5. George RE, Sanda T, Hanna M*, et al.* Activating mutations in ALK provide a therapeutic target in neuroblastoma. Nature 2008;455: 975-8.
6. Janoueix-Lerosey I, Lequin D, Brugieres L*, et al.* Somatic and germline activating mutations of the ALK kinase receptor in neuroblastoma. Nature 2008;455: 967-70.
7. Mosse YP, Laudenslager M, Longo L*, et al.* Identification of ALK as a major familial neuroblastoma predisposition gene. Nature 2008;455: 930-5.
8. Motegi A, Fujimoto J, Kotani M, Sakuraba H, Yamamoto T. ALK receptor tyrosine kinase promotes cell growth and neurite outgrowth. J Cell Sci 2004;117: 3319-29.
9. Souttou B, Carvalho NB, Raulais D, Vigny M. Activation of anaplastic lymphoma kinase receptor tyrosine kinase induces neuronal differentiation through the mitogen-activated protein kinase pathway. J Biol Chem 2001;276: 9526-31.
10. Webb TR, Slavish J, George RE*, et al.* Anaplastic lymphoma kinase: role in cancer pathogenesis and small-molecule inhibitor development for therapy. Expert Rev Anticancer Ther 2009;9: 331-56.
11. Chiarle R, Voena C, Ambrogio C, Piva R, Inghirami G. The anaplastic lymphoma kinase in the pathogenesis of cancer. Nat Rev Cancer 2008;8: 11-23.
12. McDermott U, Iafrate AJ, Gray NS*, et al.* Genomic alterations of anaplastic lymphoma kinase may sensitize tumors to anaplastic lymphoma kinase inhibitors. Cancer Res 2008;68: 3389-95.
13. De Brouwer S, De Preter K, Kumps C*, et al.* Meta-analysis of neuroblastomas reveals a skewed ALK mutation spectrum in tumors with MYCN amplification. Clin Cancer Res 2010;in press.
14. Lamant L, Pulford K, Bischof D*, et al.* Expression of the ALK tyrosine kinase gene in neuroblastoma. Am J Pathol 2000;156: 1711-21.
15. Osajima-Hakomori Y, Miyake I, Ohira M, Nakagawara A, Nakagawa A, Sakai R. Biological role of anaplastic lymphoma kinase in neuroblastoma. Am J Pathol 2005;167: 213-22.
16. Ambros PF, Ambros IM. Pathology and biology guidelines for resectable and unresectable neuroblastic tumors and bone marrow examination guidelines. Med Pediatr Oncol 2001;37: 492-504.
17. Shimada H, Chatten J, Newton WA, Jr.*, et al.* Histopathologic prognostic factors in neuroblastic tumors: definition of subtypes of ganglioneuroblastoma and an age-linked classification of neuroblastomas. J Natl Cancer Inst 1984;73: 405-16.
18. De Preter K, Speleman F, Combaret V*, et al.* Quantification of MYCN, DDX1, and NAG gene copy number in neuroblastoma using a real-time quantitative PCR assay. Mod Pathol 2002;15: 159-66.
19. Pattyn F, Speleman F, De Paepe A, Vandesompele J. RTPrimerDB: the real-time PCR primer and probe database. Nucleic Acids Res 2003;31: 122-3.
20. Hellemans J, Mortier G, De Paepe A, Speleman F, Vandesompele J. qBase relative quantification framework and software for management and automated analysis of real-time quantitative PCR data. Genome Biol 2007;8: R19.
21. Oberthuer A, Berthold F, Warnat P*, et al.* Customized oligonucleotide microarray gene expression-based classification of neuroblastoma patients outperforms current clinical risk stratification. J Clin Oncol 2006;24: 5070-8.

22. Fischer M, Skowron M, Berthold F. Reliable transcript quantification by real-time reverse transcriptase-polymerase chain reaction in primary neuroblastoma using normalization to averaged expression levels of the control genes HPRT1 and SDHA. J Mol Diagn 2005;7: 89-96.
23. Classen S, Zander T, Eggle D*, et al.* Human resting CD4+ T cells are constitutively inhibited by TGF beta under steady-state conditions. J Immunol 2007;178: 6931-40.
24. Fischer M, Bauer T, Oberthur A*, et al.* Integrated genomic profiling identifies two distinct molecular subtypes with divergent outcome in neuroblastoma with loss of chromosome 11q. Oncogene 2010;29: 865-75.
25. Falcon S, Gentleman R. Using GOstats to test gene lists for GO term association. Bioinformatics 2007;23: 257-8.
26. Oberthuer A, Hero B, Berthold F*, et al.* Prognostic impact of gene expression-based classification for neuroblastoma. J Clin Oncol 2010;28: 3506-15.
27. Caren H, Abel F, Kogner P, Martinsson T. High incidence of DNA mutations and gene amplifications of the ALK gene in advanced sporadic neuroblastoma tumours. Biochem J 2008;416: 153-9.
28. Passoni L, Longo L, Collini P*, et al.* Mutation-Independent Anaplastic Lymphoma Kinase Overexpression in Poor Prognosis Neuroblastoma Patients. Cancer Res 2009.
29. Miller JK, Shattuck DL, Ingalla EQ*, et al.* Suppression of the negative regulator LRIG1 contributes to ErbB2 overexpression in breast cancer. Cancer Res 2008;68: 8286-94.
30. Oberthuer A, Kaderali L, Kahlert Y*, et al.* Subclassification and individual survival time prediction from gene expression data of neuroblastoma patients by using CASPAR. Clin Cancer Res 2008;14: 6590-601.
31. Fischer M, Spitz R, Oberthur A, Westermann F, Berthold F. Risk estimation of neuroblastoma patients using molecular markers. Klin Padiatr 2008;220: 137-46.
32. Janoueix-Lerosey I, Schleiermacher G, Michels E*, et al.* Overall genomic pattern is a predictor of outcome in neuroblastoma. J Clin Oncol 2009;27: 1026-33.
33. Vermeulen J, De Preter K, Naranjo A*, et al.* Predicting outcomes for children with neuroblastoma using a multigene-expression signature: a retrospective SIOPEN/COG/GPOH study. Lancet Oncol 2009;10: 663-71.
34. Lo HS, Wang Z, Hu Y*, et al.* Allelic variation in gene expression is common in the human genome. Genome Res 2003;13: 1855-62.
35. Yan H, Zhou W. Allelic variations in gene expression. Curr Opin Oncol 2004;16: 39-43.
36. Zhang K, Li JB, Gao Y*, et al.* Digital RNA allelotyping reveals tissue-specific and allele-specific gene expression in human. Nat Methods 2009;6: 613-8.
37. de la Chapelle A. Genetic predisposition to human disease: allele-specific expression and low-penetrance regulatory loci. Oncogene 2009;28: 3345-8.

Legends to tables

Table 1: Summary of patient and tumor characteristics of neuroblastomas with genomic alterations of *ALK*. Allele expression indicates the numbers of wild-type (WT) and mutated (mut.) clones. Age at diagnosis is given in days. Amp, amplification; del, deletion; imb, imbalance; n.d., not done; DOD, death of disease; CR, complete remission; vgPR, very good partial remission; (*) homozygous mutation. Tumors with F1174L and R1275Q mutations are highlighted in gray.

Table 2: Summary of pair-wise comparisons of *ALK*-WT^{low}, *ALK*-WT^{high} and *ALK*^{mutated} neuroblastomas using analysis of centroid distances, ANOVA and t-test statistics. For t-test analysis and ANOVA, genes (probes) with a false discovery rate <0.05 were considered after correction for multiple testing by the Benjamini-Hochberg method.

Supplementary Table 1: Patient and tumor characteristics of the 263 neuroblastomas in this study. Indicated are the sample ID, gender (F, female; M, male), tumor stage, age (days), histological classification according to Shimada (F, favorable; UF, unfavorable; n.d., not determined), *MYCN* copy number status (1, *MYCN* not amplified as determined by FISH; amp., ≥5fold increase in *MYCN* signal numbers in relation to the numbers of chromosome 2; n.d., not determined), *ALK* mRNA expression values as log ratios according to the microarray data, and patient subgroup based on *ALK* genomic status and expression level (1, *ALK*-WT^{low}; 2, *ALK*-WT$^{intermediate\text{-}low}$; 3, *ALK*-WT$^{intermediate\text{-}high}$; 4, *ALK*-WT^{high}; 5, *ALK*^{mutated}; 6, *ALK* amplification).

Supplementary Table 2: Nucleotide sequences of the oligonucleotides used as primers in this study.

Supplementary Table 3: Relative expression levels of *ALK* in tumors with and without genomic alterations of *ALK*. The mean and median ratios as well as log ratios indicate *ALK*

expression levels in tumor subgroups in relation to the reference RNA used in the microarray experiments. In addition, the fold-change of mean and median *ALK* expression levels of the respective subgroups in comparison to tumors with WT *ALK* (top table) and in comparison to WT^{low} *ALK* neuroblastomas (bottom table) is indicated.

Supplementary Table 4: Multivariate Cox regression models based on EFS and OS considering *ALK* expression (continuous) and *ALK* mutation status (non-synonymous mutations *vs.* wild-type). Bold-face indicates statistical significance ($p<0.05$).

Supplementary Table 5: Correlation of each gene represented on the microarray with *ALK* expression levels in the subgroup harboring non-synonymous *ALK* mutations (**A**) and in the subgroup with wild-type *ALK* (**B**). Indicated are the microarray probe ID, the correlation coefficient, the ENSEMBL IDs of the respective genes and the gene symbols.

Supplementary Table 6: Results of the over-representations analysis of GO-Biological process categories by Fisher's exact test, which has been calculated for genes positively (**A**) and negatively (**B**) correlated with *ALK* expression in neuroblastomas with *ALK* mutations, or positively (**C**) and negatively (**D**) correlated with *ALK* expression in wild-type *ALK* neuroblastoma. GOBPID, Gene Ontology biological process ID; adj.PvalueBH, adjusted p-value according to the Benjamini-Hochberg method.

Legends to figures

Figure 1: Kaplan-Meier estimates for event-free and overall survival of neuroblastoma patients without (blue, n=240) and with (red, n=21) *ALK* missense mutations (EFS at 5 years, 0.71±0.03 *vs.* 0.52±0.11, p=0.040; and OS at 5 years, 0.82±0.03 *vs.* 0.62±0.11, p=0.015). The two patients harboring *ALK* amplifications were excluded from this analysis.

Figure 2: Expression levels of *ALK* in neuroblastoma subgroups defined by the genomic status of *ALK* as determined by microarray analysis (**A**). Expression levels of *ALK* in neuroblastoma subgroups defined by the genomic status of *ALK* and *ALK* mRNA levels as determined by microarray analysis (**B**). Expression values are given as log-ratios. Boxes, median expression values (horizontal line) and 25th and 75th percentiles; whiskers, distances from the end of the box to the largest and smallest observed values that are less than 1.5 box lengths from either end of the box; open circles, outlying values.

Figure 3: Kaplan-Meier estimates for event-free and overall survival of neuroblastoma patients classified according to their *ALK* expression level and the *ALK* mutation status. EFS at 5 years of *ALK*-WT^{low} (dark blue) *vs. ALK*-WT$^{intermediate\text{-}low}$ (light blue) *vs. ALK*-WT$^{intermediate\text{-}high}$ (black) *vs. ALK*-WT^{high} (green) *vs. ALK*^{mutated} (red): 0.83±0.05 *vs.* 0.73±0.06 *vs.* 0.69±0.06 *vs.* 0.59±0.07 *vs.* 0.52±0.11, respectively; OS at 5 years: 0.89±0.04 *vs.* 0.89±0.04 *vs.* 0.82±0.05 *vs.* 0.66±0.07 *vs.* 0.62±0.11, respectively. Comparison of EFS and OS of *ALK*-WT^{high} *vs. ALK*^{mutated}, p=0.546 and p=0.652, respectively.

Figure 4: Principle component analysis (PCA) of gene expression profiles from *ALK*-WT^{low} (light blue), *ALK*-WT^{high} (dark blue) and *ALK*^{mutated} (green) neuroblastomas as well as tumors with *ALK* amplification (pink).

Supplementary figure 1: Kaplan-Meier estimates for event-free and overall survival of neuroblastoma patients with a normal genomic *ALK* status (blue), F1174L mutation (red),

R1275Q mutation (green), or other *ALK* mutations (black). Pair-wise comparisons revealed no significant differences in the clinical courses between subgroups harboring different types of *ALK* mutations.

Supplementary figure 2: Correlation of *ALK* log expression values in 81 samples as determined by microarray and RT-qPCR (Pearson correlation coefficient, r=0.85).

Supplementary figure 3: Western blot analysis of ALK and of the phosphorylated ALK targets p-STAT3, p-AKT and p-ERK1/2 in primary neuroblastomas. The sample ID, the genomic status of *ALK* and *ALK* mRNA expression levels according to the classification into percentiles (see text) are indicated above the blot results: +++, very high *ALK* mRNA expression according to amplified *ALK*; ++, high *ALK* expression according to *ALK*-WT^{high}; +, intermediate-high *ALK* expression levels according to *ALK*-WT$^{intermediate\text{-}high}$; (+), intermediate-low *ALK* expression levels according to *ALK*-WT$^{intermediate\text{-}low}$; -, low *ALK* expression levels according to *ALK*-WT^{low}.

Supplementary figure 4: Kaplan-Meier estimates for event-free and overall survival of neuroblastoma patients classified according to their *ALK* expression level and the *ALK* mutation status after exclusion of patients with *MYCN* amplified tumors. EFS at 5 years of *ALK*-WT^{low} (dark blue) *vs.* *ALK*-WT$^{intermediate\text{-}low}$ (light blue) *vs.* *ALK*-WT$^{intermediate\text{-}high}$ (black) *vs.* *ALK*-WT^{high} (green) *vs.* *ALK*^{mutated} (red): 0.89±0.04 *vs.* 0.81±0.06 *vs.* 0.69±0.06 *vs.* 0.65±0.08 *vs.* 0.67±0.12, respectively; OS at 5 years: 0.96±0.03 *vs.* 0.96±0.03 *vs.* 0.84±0.05 *vs.* 0.74±0.07 *vs.* 0.80±0.10, respectively. Comparison of EFS and OS of *ALK*-WT^{high} *vs.* *ALK*^{mutated}, p=0.88 and p=0.65, respectively.

Supplementary figure 5: Principle component analysis (PCA) of gene expression profiles from *ALK*-WT^{low} (light blue), *ALK*-WT^{high} (dark blue) and *ALK*^{mutated} neuroblastomas (green and red) after exclusion of *MYCN* amplified tumors. Tumors with *ALK* mutations and high

ALK expression are indicated in green, whereas the four *ALK* mutated tumors having intermediate or low *ALK* expression are indicated in red.

Supplementary figure 6: Western blot analysis of ALK, phosphorylated ALK and the phosphorylated ALK targets p-STAT3, p-AKT and p-ERK1/2 in transgenic SK-N-AS cells harboring either WT *ALK* (WT), F1174L mutant *ALK* (FL), R1275Q mutant *ALK* (RQ) or GFP as a control. Results are shown for two clones per transgenic cell line before and after induction of the transgene by addition of tetracycline.

Supplementary figure 7: Expression of *PTN* and *MDK* in neuroblastoma subgroups defined by the genomic status of *ALK* and *ALK* mRNA levels as determined by microarray analysis (**A**). Correlation of *PTN* and *MDK* expression with *ALK* mRNA levels in WT *ALK* neuroblastomas (**B**). Expression values are given as log-ratios. Boxes, median expression values (horizontal line) and 25th and 75th percentiles; whiskers, distances from the end of the box to the largest and smallest observed values that are less than 1.5 box lengths from either end of the box; open circles, outlying values.

Patient	exon	mutation (DNA)	allele expression (WT/mut.)	mutation (protein)	known	germline	stage	age	*MYCN*	1p	11q	outcome
NB49529	21	3383 G>C	4/5	G1128A	yes	n.d.	3	423	amp	del1p	no	DOD
NB374	22	3509 T>C	6/4	I1170T	no	n.d.	1	887	no	no	no	CR
NB068	22	3509 T>G	3/7	I1170S	no	n.d.	4S	121	no	no	no	CR
NB166	22	3452 C>T	1/9	T1151M	yes	no	3	344	no	no	no	CR
NB005	22	3452 C>T	9/0	T1151M	yes	n.d.	4	521	no	no	no	PR
NB531	23	3600 G>A*	n.d.	silent	no	n.d.	2a	114	no	no	no	CR
NB092	23	3594 C>T	n.d.	silent	no	no	4	942	no	no	del11q	vgPR
NB091	23	3521 T>G	7/2	F1174C	yes	no	2b	507	no	no	no	CR
NB149	23	3522 C>G	9/0	F1174L	yes	n.d.	1	498	no	no	no	CR
NB086	23	3522 C>A	10/2	F1174L	yes	no	4	8983	no	no	no	DOD
NB113	23	3522 C>G	9/4	F1174L	yes	n.d.	1	744	no	no	no	CR
NB111	23	3522 C>A	8/4	F1174L	yes	n.d.	3	243	no	no	no	CR
NB333	23	3522 C>A	11/3	F1174L	yes	n.d.	4	536	amp	del1p	no	DOD
NB602	24	3733 T>G	4/6	F1245V	no	no	3	1585	no	imb1p	no	DOD
NB49107	24	3718 T>G	7/3	L1240V	no	no	4	3749	amp	no	no	CR
NB643	25	3824 G>A	8/8	R1275Q	yes	n.d.	2a	374	no	no	no	CR
NB504	25	3824 G>A	7/9	R1275Q	yes	no	4	517	amp	del1p	no	DOD
NB326	25	3824 G>A	9/1	R1275Q	yes	no	4	2105	amp	imb1p	no	DOD
NB052	25	3824 G>A	9/3	R1275Q	yes	n.d.	4S	147	no	no	no	CR
NB134	25	3824 G>A	10/3	R1275Q	yes	n.d.	3	541	no	no	no	CR
NB132	25	3824 G>A	9/1	R1275Q	yes	no	1	479	no	no	no	CR
NB501	25	3824 G>A	4/11	R1275Q	yes	no	3	1017	amp	imb1p	del11q	DOD
NB331	25	3824 G>A	5/9	R1275Q	yes	n.d.	4	1841	no	del1p	no	DOD
NB276		amp				n.d.	3	379	amp	del1p	no	DOD
NB49368		amp				n.d.	4	710	amp	imb1p	n.d.	CR

	ALK mutated vs. ALK WT^{low}	ALK mutated vs. ALK WT^{high}	ALK WT^{low} vs. ALK WT^{high}
centroid distance (p-value)	<0.001	0.027	<0.001
ANOVA (genes)	173	1	562
t-test (genes)	1567	25	341

Fig. 1

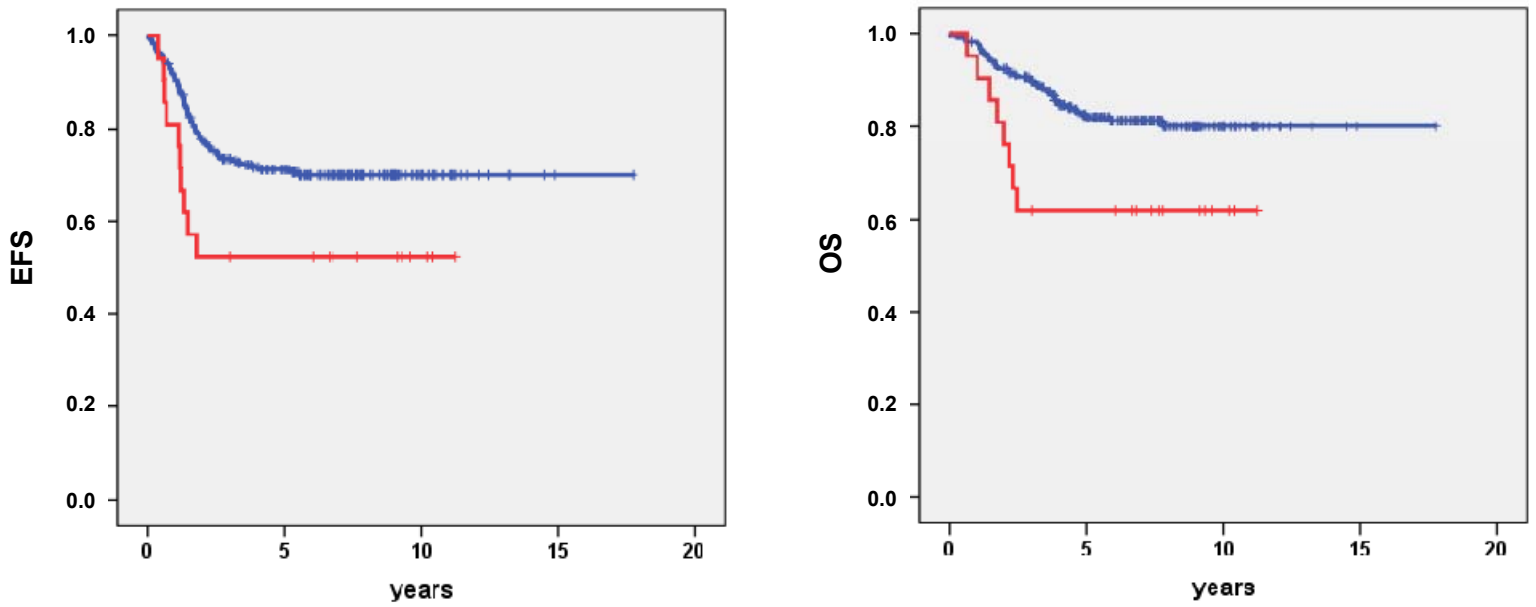

Fig. 2A

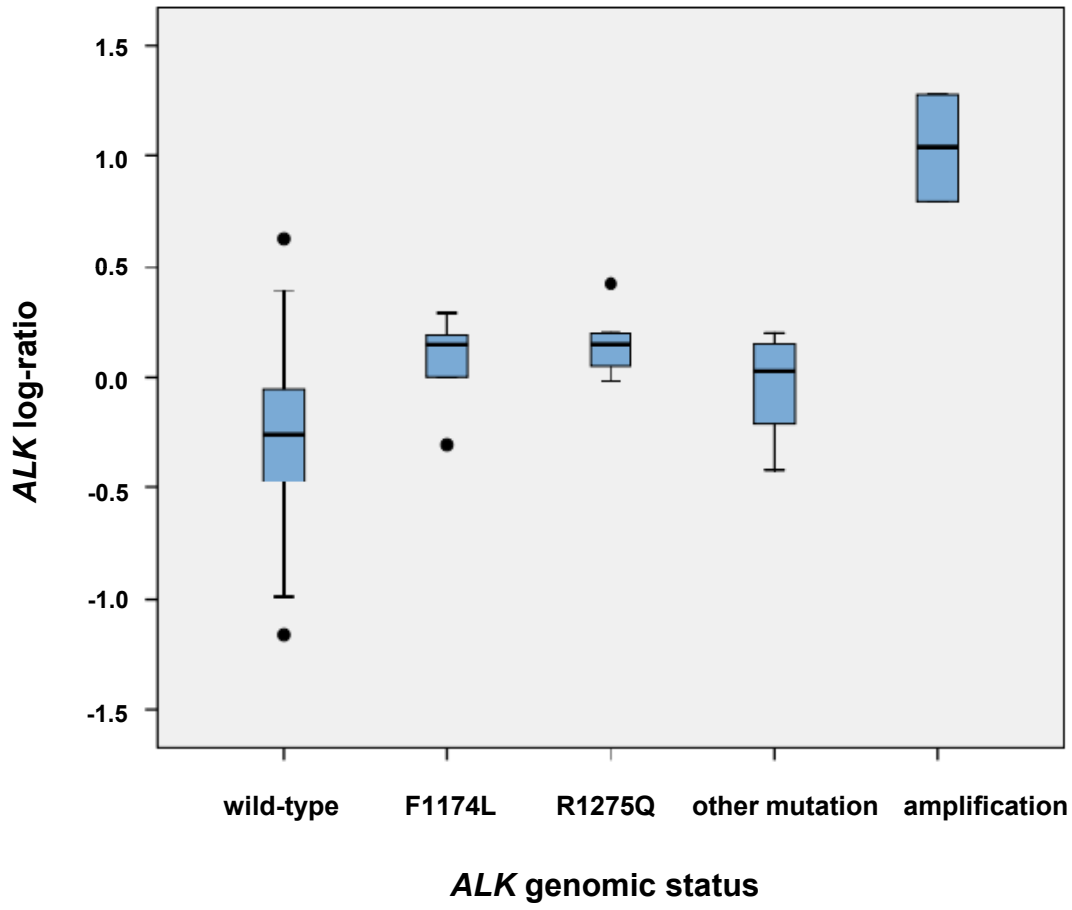

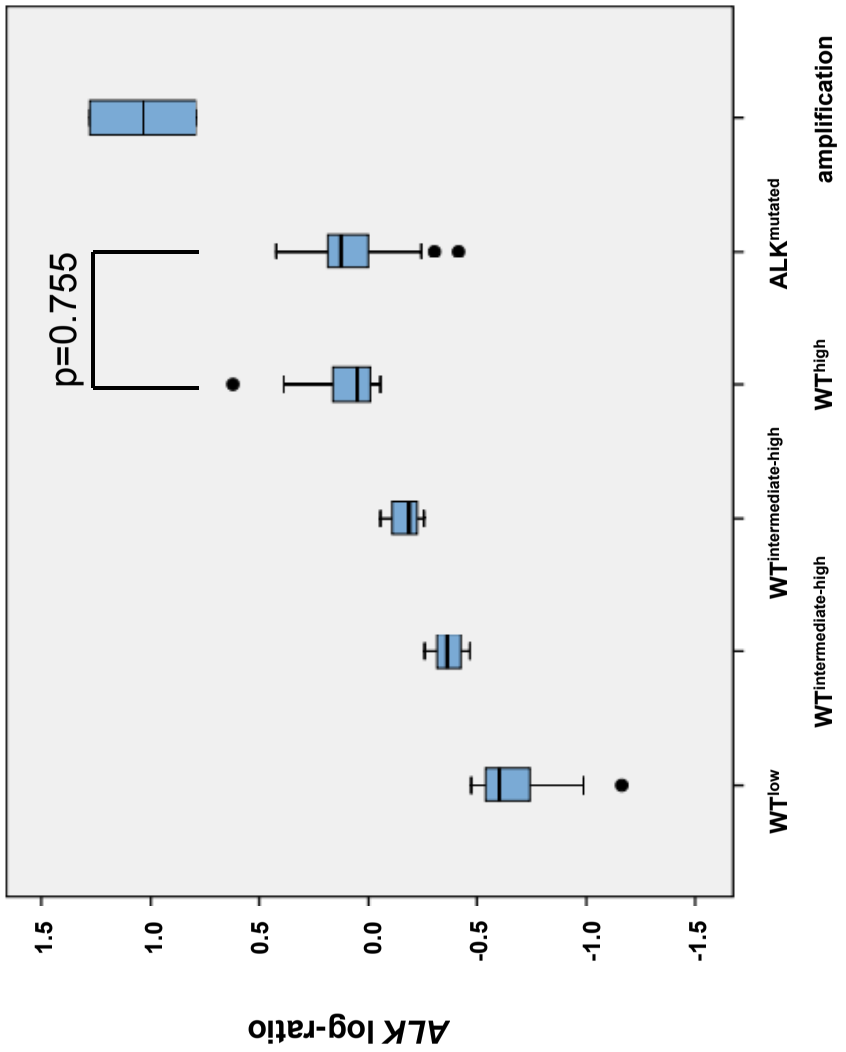

Fig. 2B

Fig. 3

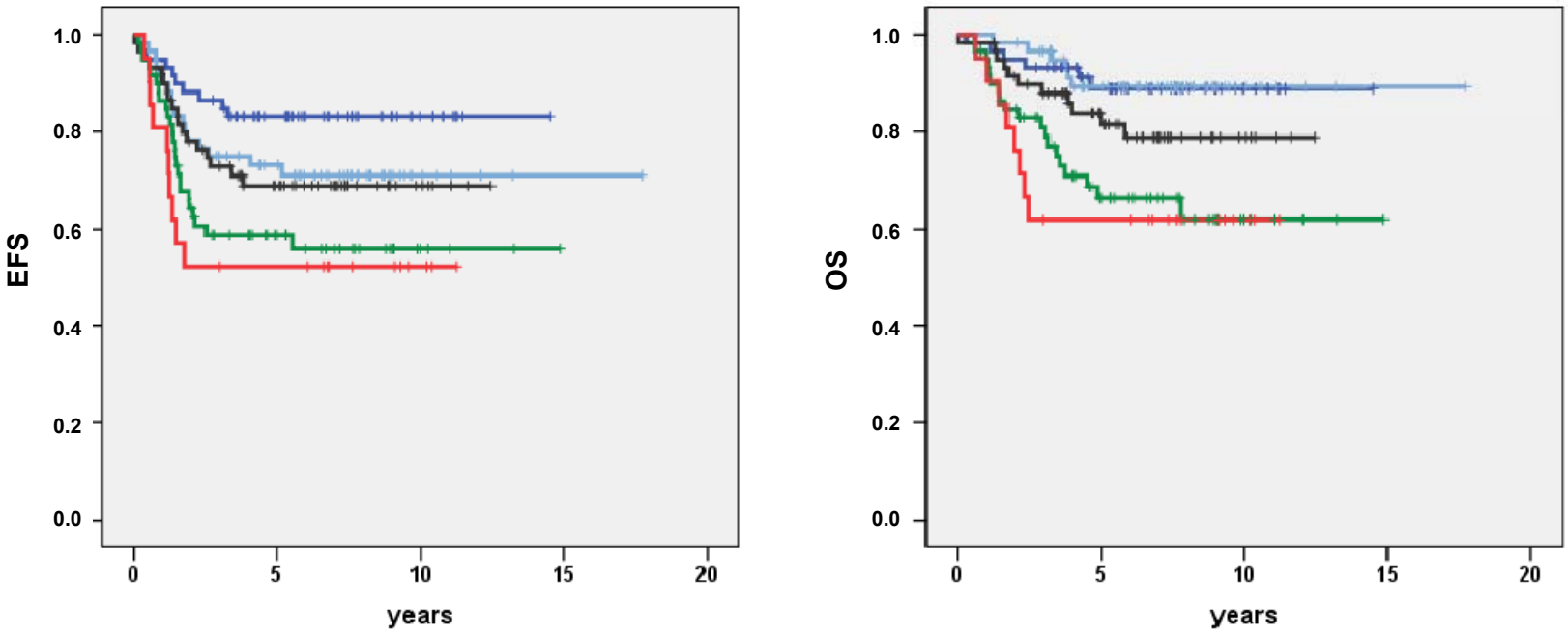

Fig. 4

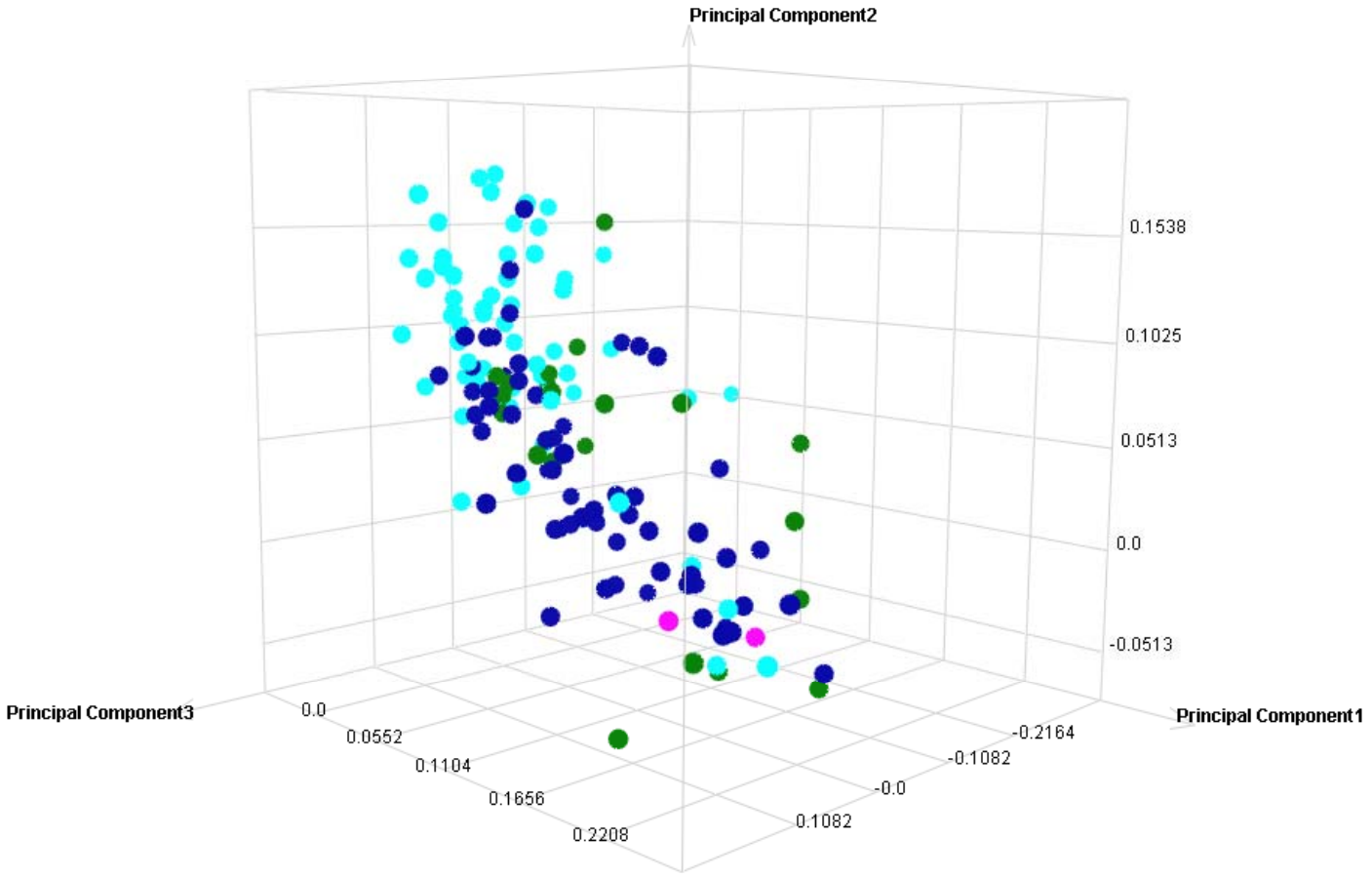

Supplementary Fig. 1

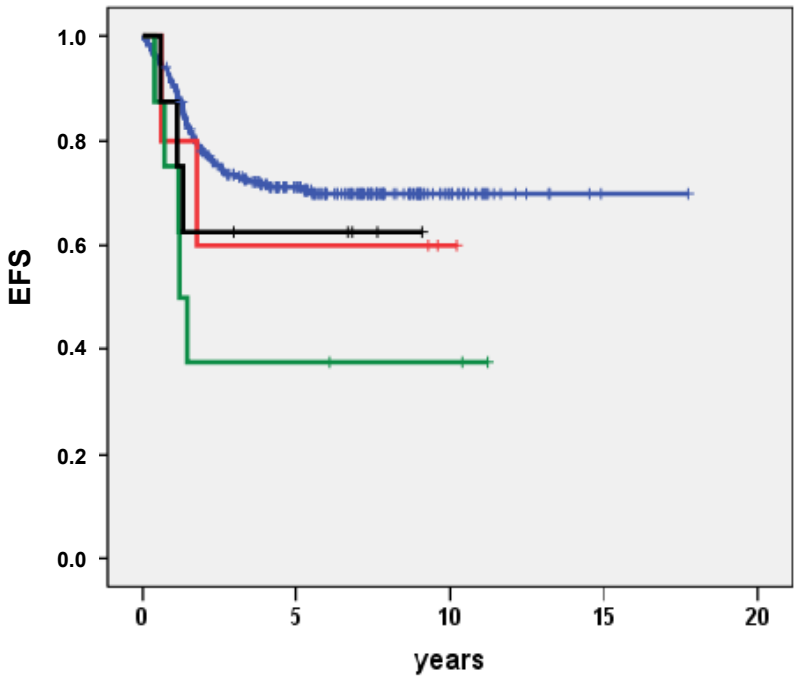

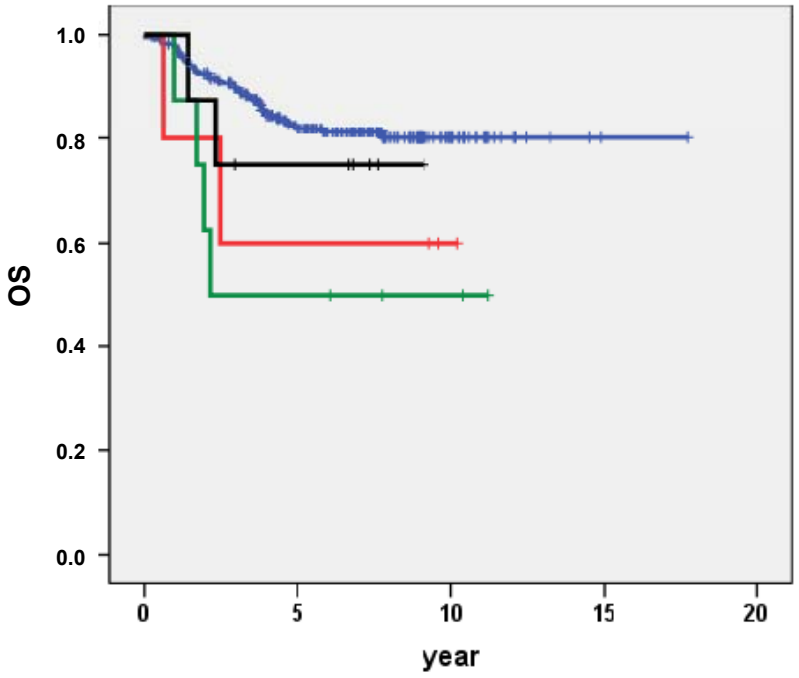

Supplementary Fig. 2

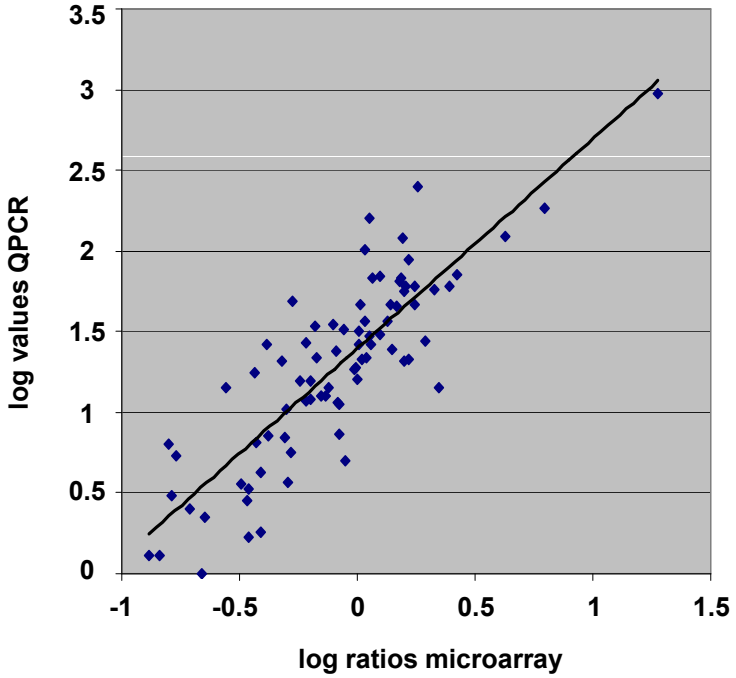

Supplementary Fig. 3

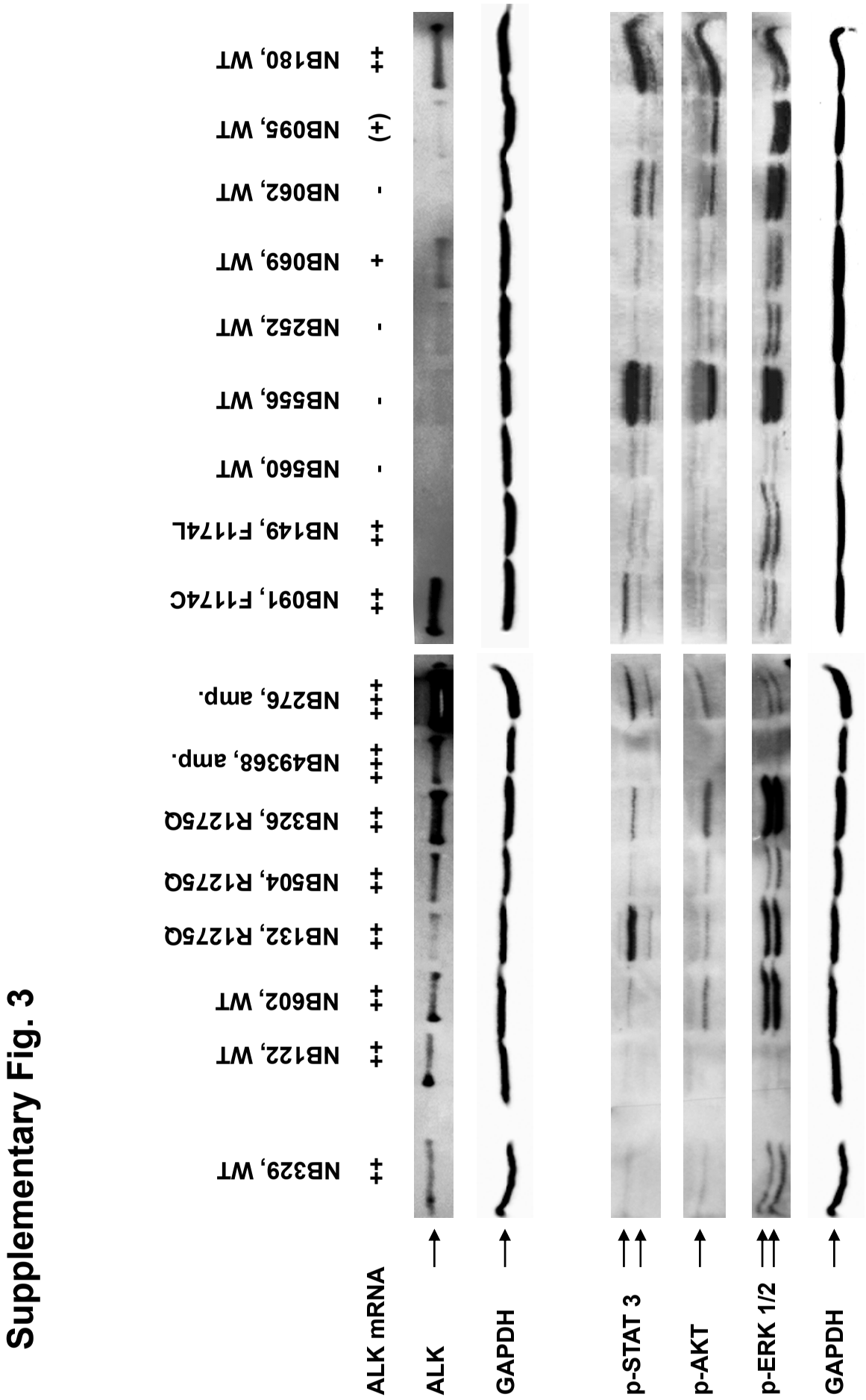

Supplementary Fig. 4

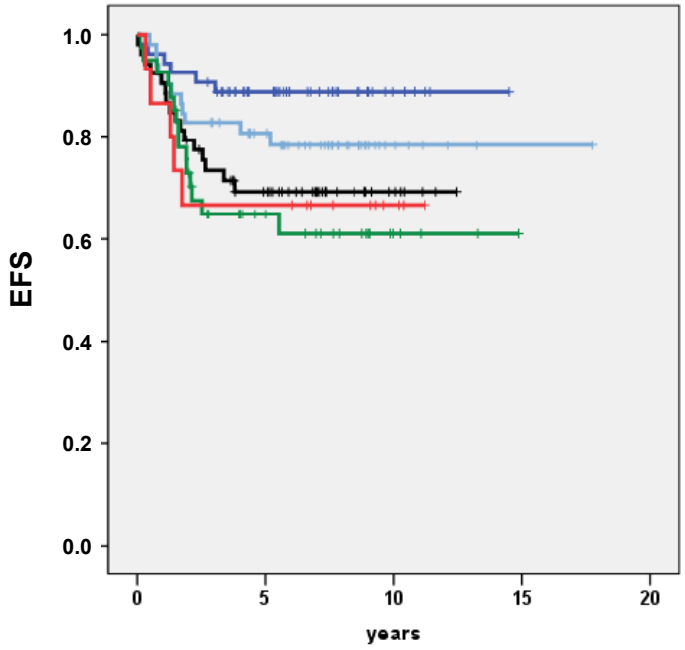

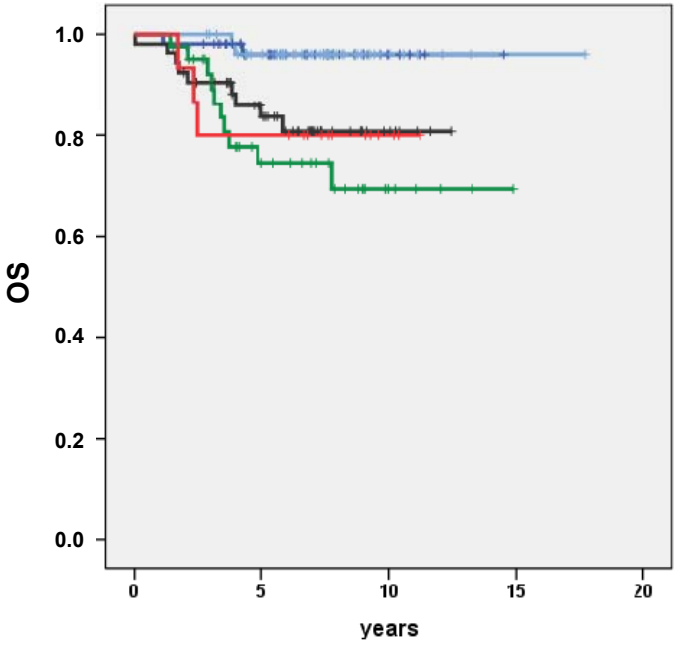

Supplementary Fig. 5

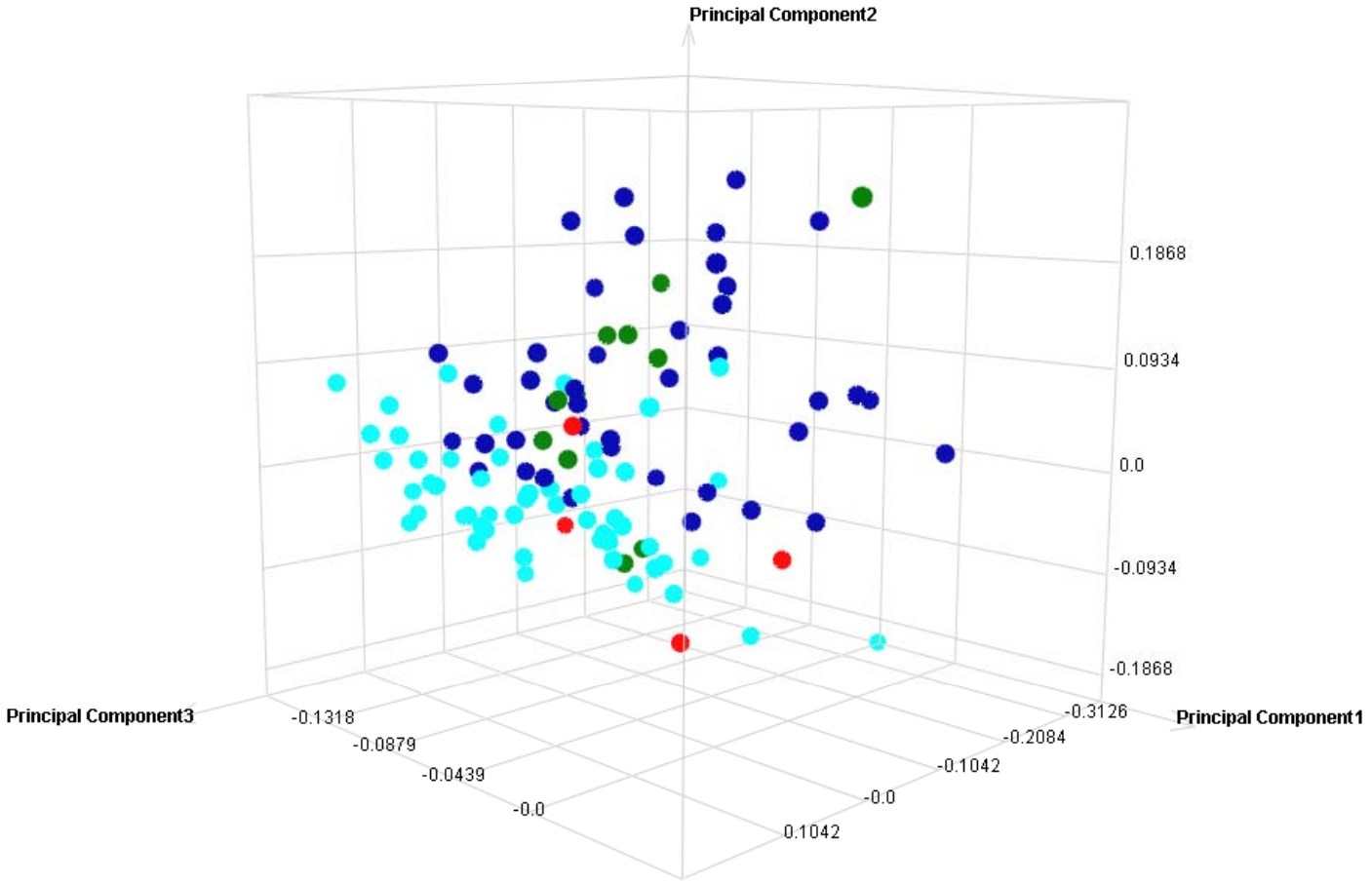

Supplementary Fig. 6

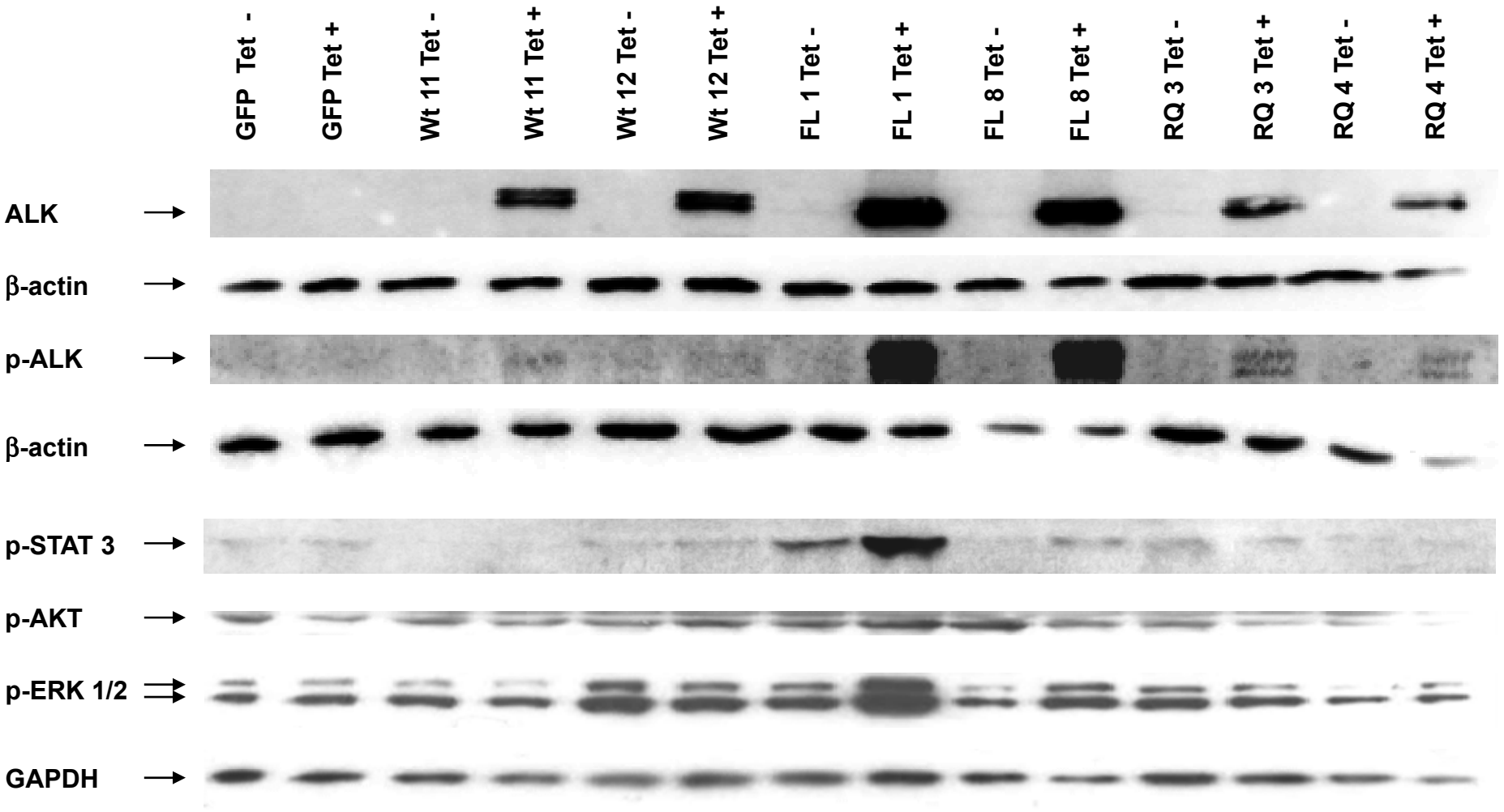

Supplementary Fig. 7A

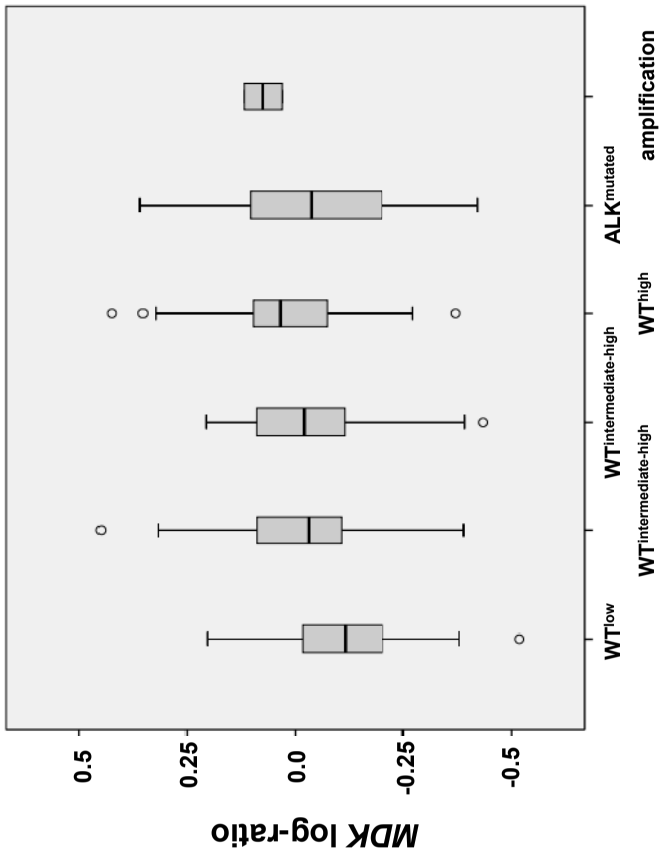

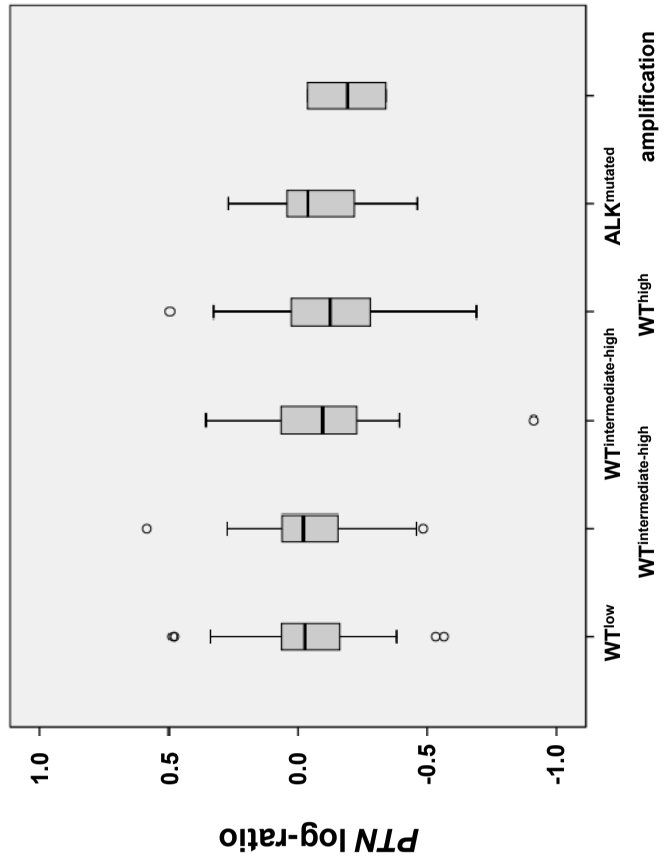

Supplementary Fig. 7B